3C Protease as Ferroptosis Inducer

Subjects: Cell Biology

Contributor: Alexey Komissarov

Regulated cell death (RCD) is a fundamental process common to nearly all living beings and essential for the development and tissue homeostasis in animals and humans. A wide range of molecules can induce RCD including a number of viral proteolytic enzymes. To date, numerous data indicate that picornaviral 3C proteases can induce RCD. In most reported cases, these proteases induce classical caspase-dependent apoptosis. In contrast, the human hepatitis A virus 3C protease (3Cpro) has recently been shown to cause caspase-independent cell death accompanied by previously undescribed features.

In the current topic the results of the study where 3Cpro-induced cell death was characterized morphologically and biochemically are presented. It was found that dead cells demonstrated necrosis-like morphological changes including permeabilization of plasma membrane, loss of mitochondrial potential, as well as mitochondria and nuclei swelling. Additionally, it was shown that 3Cpro-induced cell death was efficiently blocked by ferroptosis inhibitors and was accompanied by intense lipid peroxidation. Taken together, these results indicate that 3Cpro induces ferroptosis upon its individual expression in human cells. This is the first demonstration that a proteolytic enzyme can induce ferroptosis, the recently discovered and actively studied type of RCD.

hepatitis A virus | 3C protease | regulated cell death | ferroptosis | ectopic expression

1. Introduction

Regulated cell death (RCD) is a fundamental physiological process common to nearly all living beings [1]. In animals and humans, RCD is crucial for the development and tissue homeostasis, while abnormal RCD causes a wide range of diseases [2]. The mechanisms of cell death have been studied for more than 50 years, and today, more than ten RCD types are discriminated according to their inducers, key meditators, and cell morphology during and after death [3].

A wide range of molecules can induce RCD including certain viral proteolytic enzymes. Similar to other virus proteins, viral proteases are multifunctional. In addition to the main function of processing viral proteins, they can cleave cellular proteins. This can inhibit the transcription of cellular genes and cellular mRNA translation, block nuclear transport, and suppress the antiviral immune response [4][5]. Acting on cellular proteins, viral proteases can trigger RCD.

To date, numerous data indicate the ability of picornaviral 3C proteases to induce RCD. In most reported cases, these proteases induce classical caspase-dependent apoptosis [6][7][8]. In contrast, the rhinovirus 3C protease induces caspase-independent cell death; however, the underlying mechanism remains unclear [9]. Previously, we

demonstrated that hepatitis A virus 3C protease (3Cpro) induces cell death that is also independent of caspase activity and features a unique cell morphology, specifically, the accumulation of cytoplasmic vacuoles with previously undocumented features. This suggested that the 3Cpro-induced cell death proceeds by an unknown pathway or is a new variant of a known RCD type [10][11][12].

2. Ectopic Expression of 3Cpro and Its Inactive Form 3Cmut in Human Cells

Two genetic constructs were derived from the pCI vector: pCI-3C for the constitutive expression of active hepatitis A virus 3C protease (3Cpro) and pCI-3Cmut expressing the mutant enzyme with no proteolytic activity due to the Cys172-Ala substitution in the active site (3Cmut) (**Figure 1**A) [13][14]. HEK293, HeLa, and A549 cells were transfected with these genetic constructs, and 15 h post transfection (p.t.), the expression of the corresponding genes was confirmed by immunoblotting with antibodies against 3Cmut (**Figure 1**B). The 3Cpro production in HEK293 cells was higher compared to the other cell lines, since the 3Cpro level detected by immunoblotting [15] in the lysate of a smaller number of cells was comparable to that in HeLa and A549 cells.

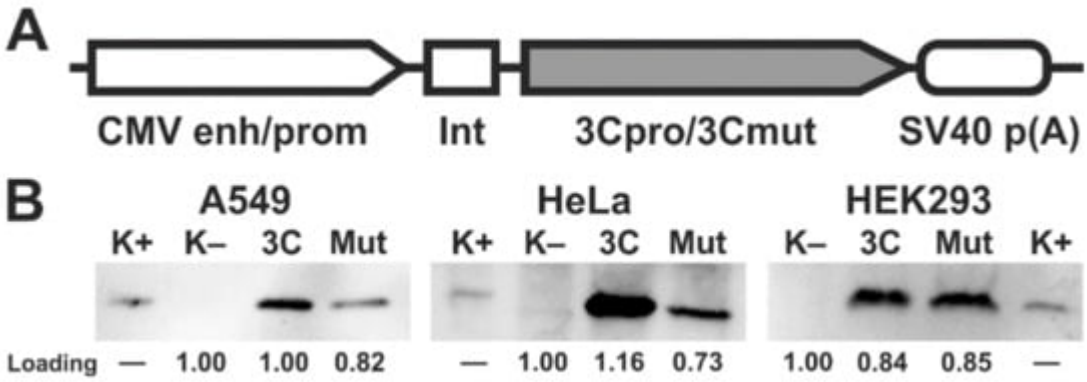

Figure 1. Expression of 3Cpro and its inactive form 3Cmut in human cells. (**A**) Expression cassettes in pCI-3C and pCI-3Cmut. CMV enh/prom, cytomegalovirus immediate-early enhancer/promoter; Int, chimeric human b-globin/IgG intron; 3Cpro/3Cmut, human hepatitis A virus 3C protease (intact or mutant, respectively) gene; SV40 p(A), late mRNA polyadenylation signal of SV40. (**B**) Analysis of 3Cpro and 3Cmut expression in HEK293, HeLa, and A549 cells by immunoblotting 15 h p.t.; 3C/Mut, lysate of cells transfected with pCI-3C/pCI-3Cmut; K–, lysate of non-transfected cells; K+, recombinant 3Cmut (1 ng). The lysates were prepared from 200,000 HEK293 or 500,000 HeLa/A549 cells. “Loading” shows the relative total protein per track estimated for each cell line using the stain-free technology.

3. 3Cpro Expression Induces Caspase-Independent Cell Death with Cytoplasmic Vacuolization

The cytotoxic effect after the transfection with pCI-3C/pCI-3Cmut was analyzed. The expression of mutant protease 3Cmut induced no cytotoxic effect (**Figure 2**A; solid lines). At the same time, the proportion of living cells

in cultures expressing active 3Cpro decreased 15 h p.t. to reach the minimum 18 h p.t. (about 25% for HEK293 and less than 5% for HeLa and A549) and remained stable up to the end of the observation period (24 h p.t.) (**Figure 2**A; dashed lines).

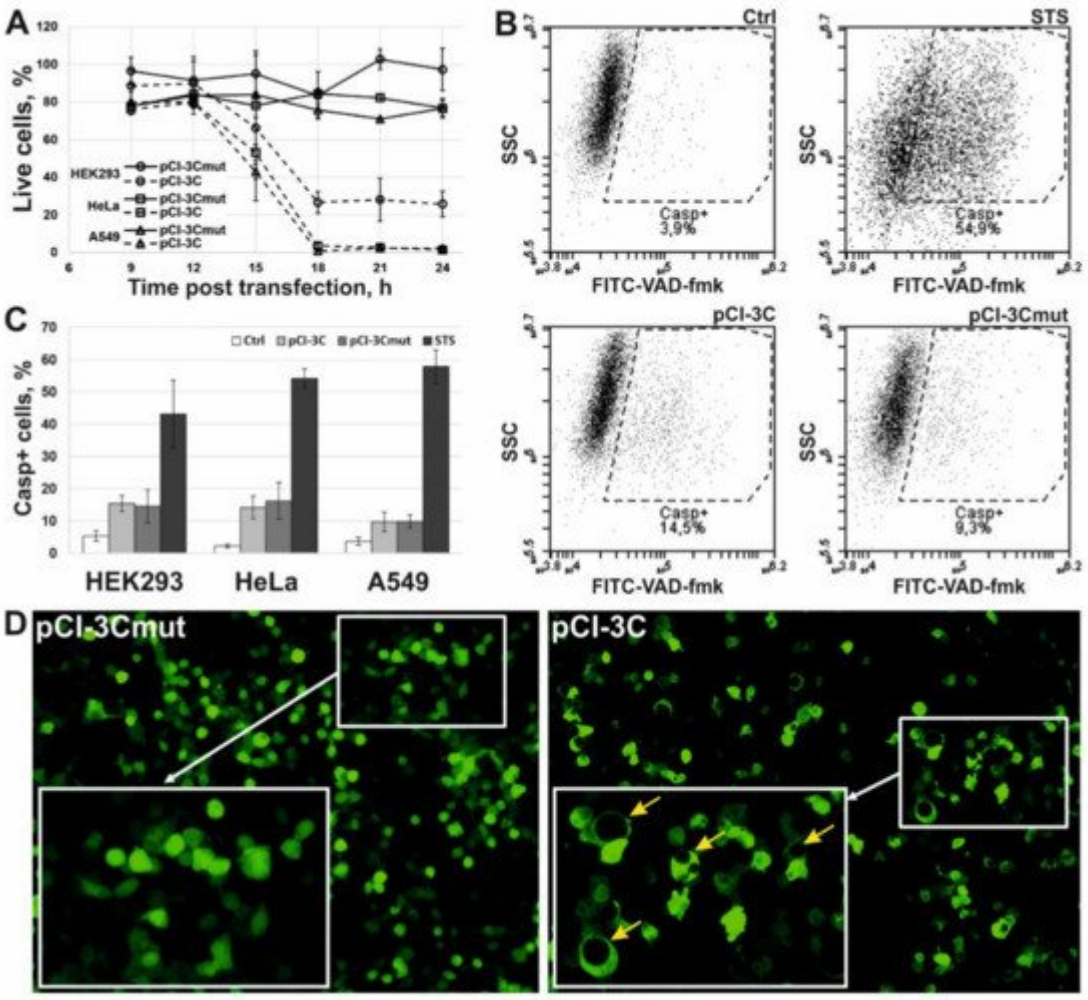

Figure 2. Effects of ectopic 3Cpro expression in HEK293, HeLa, and A549 cells. (**A**) Cytotoxic effect induced by 3Cpro expression. Results are expressed as the percentage of viable cells relative to non-transfected cells. (**B**) Representative flow cytometry images of non-transfected HeLa cells (Ctrl) and those transfected with pCI-3C and pCI-3Cmut, or incubated with 1 µM staurosporine (STS) and stained with FITC-conjugated caspase inhibitor (FITC-VAD-fmk). SSC, side scatter. (**C**) Caspase activation analysis using FITC-VAD-fmk in non-transfected cells (Ctrl) and those transfected with pCI-3C/pCI-3Cmut or incubated with STS. (**D**) Vacuolization of cells expressing 3Cpro. HEK293 cells were co-transfected with pCI-3Cmut (left) or pCI-3C (right) together with pCI-EGFP (1:1 by weight) and analyzed by fluorescence microscopy 24 h p.t. Yellow arrows indicate cells with vacuoles. All values are represented as mean ± SD of two independent experiments with triplicates (n = 6).

The involvement of caspases in the 3Cpro-induced cell death was evaluated using the fluorescent caspase inhibitor FITC-VAD-fmk (**Figure 2**B). The proportion of cells with active caspases was about 15% after the transfection with either pCI-3C or pCI-3Cmut as demonstrated by flow cytometry (**Figure 2**C). At the same time, a considerable fraction of control cells treated with staurosporine (STS, a protein kinase C inhibitor, a well

characterized inductor of caspase-dependent apoptosis [16]), showed the activation of caspases, which demonstrates that all the cell lines used are prone to caspase-dependent apoptosis. Thus, the data obtained confirm that the cytotoxic effect of 3Cpro depends on the proteolytic activity and the cell death is not accompanied by the activation of caspases.

We have also confirmed that 3Cpro-induced cell death is accompanied by cytoplasmic vacuolization as previously demonstrated [11]. Thus, a considerable fraction of HEK293 cells co-transfected with pCI-3C/pCI-3Cmut and pCI-EGFP (expressing the enhanced green fluorescent protein) showed green fluorescence 24 h p.t. as well as cytoplasmic vacuolization (**Figure 2**D; right). Nearly no cells were demonstrating green fluorescence 48 h p.t. At the same time, no cytoplasmic vacuolization was observed after co-transfection with pCI-3Cmut and pCI-EGFP, and cells remained attached to the substrate and emitted green fluorescence up to the end of the observation period (72 h p.t.) (**Figure 2**D; left). In the case of HeLa and A549, most cells transfected with pCI-3C/pCI-EGFP died 24 h p.t., and individual survived cells demonstrated green fluorescence but no cytoplasmic vacuolization. The data obtained likely indicate a higher susceptibility of HeLa and A549 cells to 3Cpro-induced cell death compared to HEK293. However, these data do not allow concluding about the cytoplasmic vacuolization in HeLa and A549 cells, since the vacuoles can be visualized only in EGFP-contrasted cytoplasm, while cells seem to die before they accumulate sufficient quantity of EGFP.

Thus, the effect of 3Cpro on human cells in the pCI-based expression system in vitro is similar to that previously reported by us [10][11].

4. Cells Expressing 3Cpro Acquire Necrotic Morphology and Are Characterized by Nuclei and Mitochondria Swelling

The morphology of HEK293, HeLa, and A549 cells transfected with pCI-3C or pCI-3Cmut was analyzed by staining with 1,1′,3,3,3′,3′-hexamethylindodicarbo-cyanine iodide (DiIC1(5)) and propidium iodide (PI) at different times p.t. to evaluate the mitochondrial metabolic activity and the plasma membrane integrity, respectively (**Figure 3**A). The vast majority of the cells expressing inactive 3Cmut at all time points had active mitochondria and intact plasma membrane, which are indicative of living cells (**Figure 3**B; 3Cmut). As active 3Cpro was expressed in culture, the proportion of living cells gradually decreased, and the proportion of cells with functionally inactive mitochondria and disrupted plasma membrane (i.e., with necrotic morphology) proportionally increased; at the same time, the proportions of other cell populations remained largely unaltered (**Figure 3**B; 3Cpro).

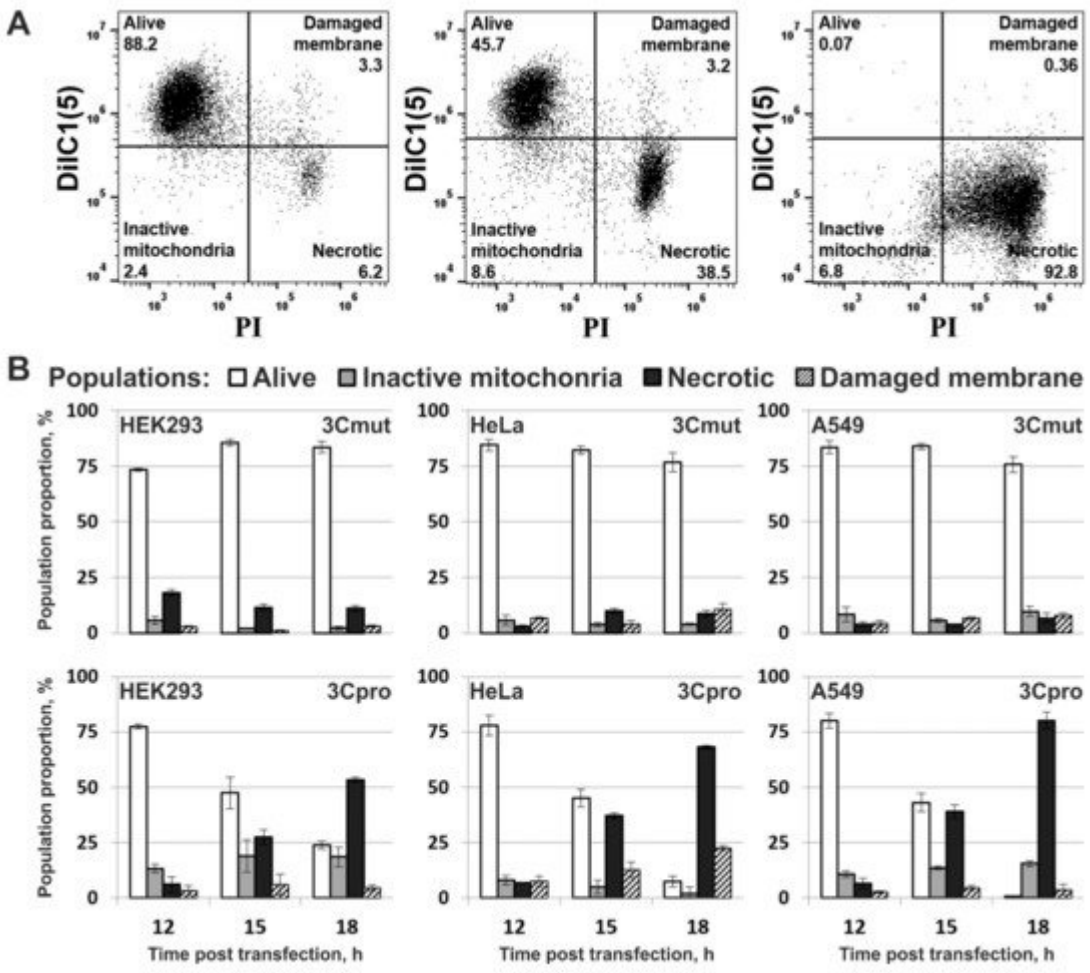

Figure 3. Flow cytometry analysis of morphology of 3Cpro expressing cells. (**A**) Representative dot plots of A549 cells stained with mitochondrial membrane potential sensitive dye 1,1′,3,3,3′,3′-hexamethylindodicarbo-cyanine iodide (DiIC1(5)) and propidium iodide (PI) 12 (left), 15 (middle), and 18 (right) h p.t. with pCI-3C. (**B**) Morphological changes in cell cultures expressing 3Cmut or 3Cpro. The proportions of different cell subpopulations discriminated on the basis of DiIC1(5) and PI staining are shown. All values are represented as mean ± SD of two independent experiments with triplicates (n = 6).

The morphology of nuclei and mitochondria in the 3Cpro-expressing cells was analyzed using fluorescence microscopy (representative pictures are presented for HeLa cells in **Figure 4**). For this purpose, DNA was stained with Hoechst 33342. Since the results of the experiment shown in **Figure 3** indicated that 3Cpro-expressing cells lose mitochondrial membrane potential, mitochondria were visualized by immunostaining with anti-AIF and fluorescently labeled antibodies. Cells expressing inactive 3Cmut demonstrated normal nuclear and mitochondrial morphology (**Figure 4**, 3Cmut), whereas those expressing 3Cpro demonstrated partial chromatin condensation, as well as hypertrophy and rounding of their nuclei and mitochondria, indicating their swelling (**Figure 4**, 3Cpro).

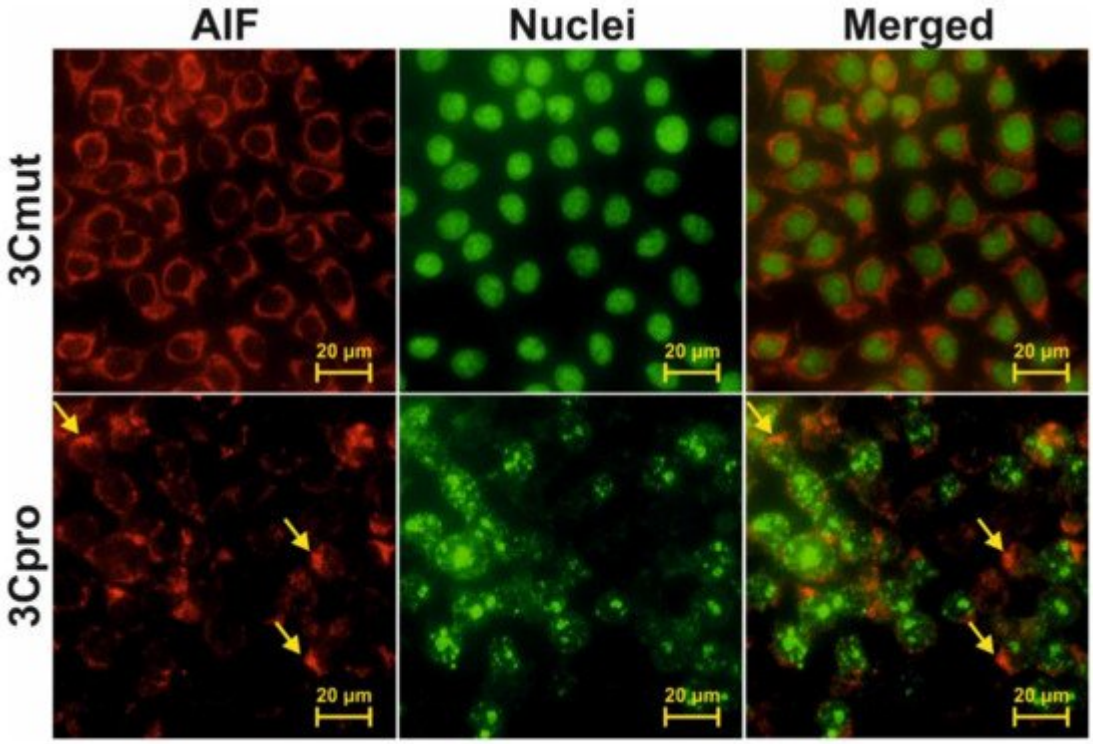

Figure 4. Analysis of nuclear and mitochondrial morphology in cells expressing 3Cpro. HeLa cells 18 h p.t. with pCI-3Cmut (3Cmut) or pCI-3C (3Cpro) were fixed and the mitochondrial protein AIF was visualized using AlexaFluor 568-labelled antibodies (AIF), while the nuclei were stained with Hoechst 33342 (Nuclei) as described in the Materials and Methods section. Arrows indicate aggregates of swollen mitochondria.

5. 3Cpro-Induced Cell Death Is Effectively Blocked by Ferroptosis Inhibitors and Is Accompinied by Lipid Peroxidation

The necrotic morphology acquired by 3Cpro-expressing cells is typical of several RCD types: necroptosis, parthanatos, MPT-associated death, and ferroptosis. We examined the effect of their inhibitors on the cytotoxic effect of 3Cpro by analyzing the mitochondrial potential in transfected cell cultures, which is correlated with plasma membrane integrity according to the results shown in **Figure 3**. The presence of necrostatin-1 (Nec1, necroptosis inhibitor [17]), PJ34 (parthanatos inhibitor [18]), and cyclosporin A (CsA, inhibitor of MPT-associated death [19]) had no effect on the survival of 3Cpro-expressing cells (**Figure 5**A–C, Nec1, PJ34, and CsA). On the contrary, lipophilic antioxidant ferrostatin-1 (Fer1) and iron chelator desferrioxamine (DFO), common ferroptosis inhibitors [20][21][22], efficiently blocked the death of cells transfected with pCI-3C (**Figure 5**A–C, Fer1 and DFO), as well as those exposed to 50 µM erastin (**Figure 5**D)—the well-known ferroptosis inducer [23][24].

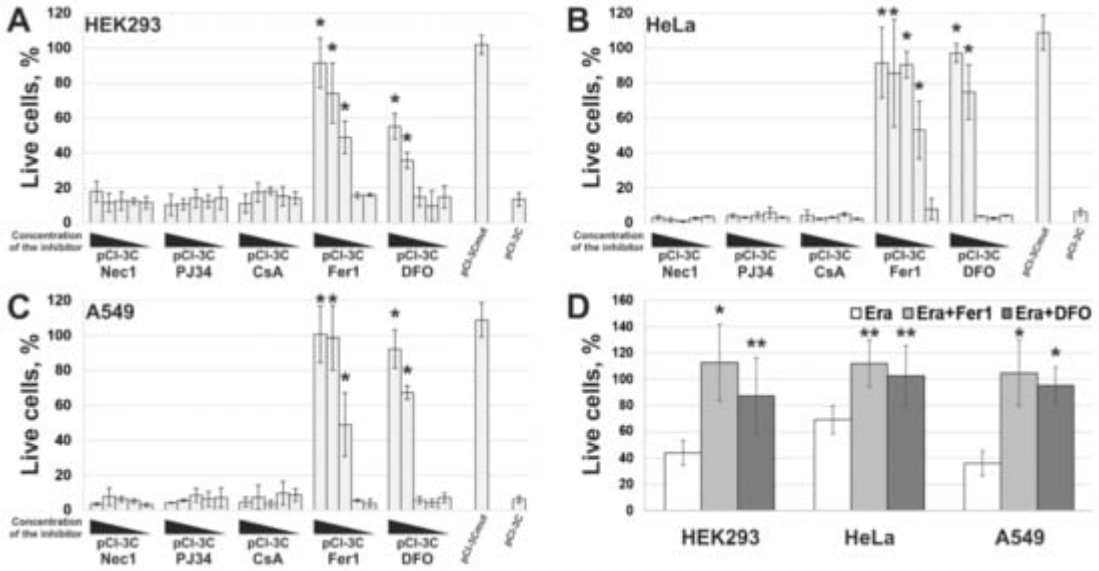

Figure 5. Effect of RCD inhibitors on 3Cpro-induced cell death. HEK293 (**A**), HeLa (**B**), and A549 (**C**) cells were transfected with pCI-3Cmut, or pCI-3C, or transfected with pCI-3C and exposed to different concentrations of necrostatin-1 (Nec1, 5000–0.5 μM), PJ34 (50–0.005 μM), cyclosporin A (CsA, 1000–0.1 μM), ferrostatin-1 (Fer1, 200–0.02 μM), and desferrioxamine (DFO, 10,000–1 μM). The viability of cells was analyzed 18 h p.t. as described in the Materials and Methods section, and the results were presented as the percentage of viable cells relatively to non-transfected cells. (**D**) Ferroptosis induction in the cell lines used. Cells were exposed to erastin (Era) alone or together with Fer1 (Era + Fer1) or DFO (Era + DFO). All values are represented as mean ± SD of two independent experiments with triplicates. Statistically significant differences between cells treated with indicated inhibitors and untreated cells (**A**–**C**), or between cells treated with Era alone and with Fer1/DFO (**D**) are marked with asterisks (Mann–Whitney U-test, $n = 6$, * $p < 0.01$, ** $p < 0.05$).

Lipid peroxidation is one of the key markers of ferroptosis. We analyzed this process in cells using BODIPY 581/591 C11 reagent which fluorescence, upon oxidation, shifts from red to green, providing a robust indication of lipid peroxidation. We found that both non-transfected cells and those transfected with pCI-3Cmut demonstrated predominantly red fluorescence, thus indicating the preponderance of the reduced form of BODIPY (**Figure 6**, Ctrl and 3Cmut, respectively). At the same time, cells expressing 3Cpro were characterized by the significant shift toward green fluorescence similar to the cells with induced lipid peroxidation due to cumene hydroperoxide exposure. These data indicate that 3Cpro-induced cell death is accompanied by intense lipid peroxidation.

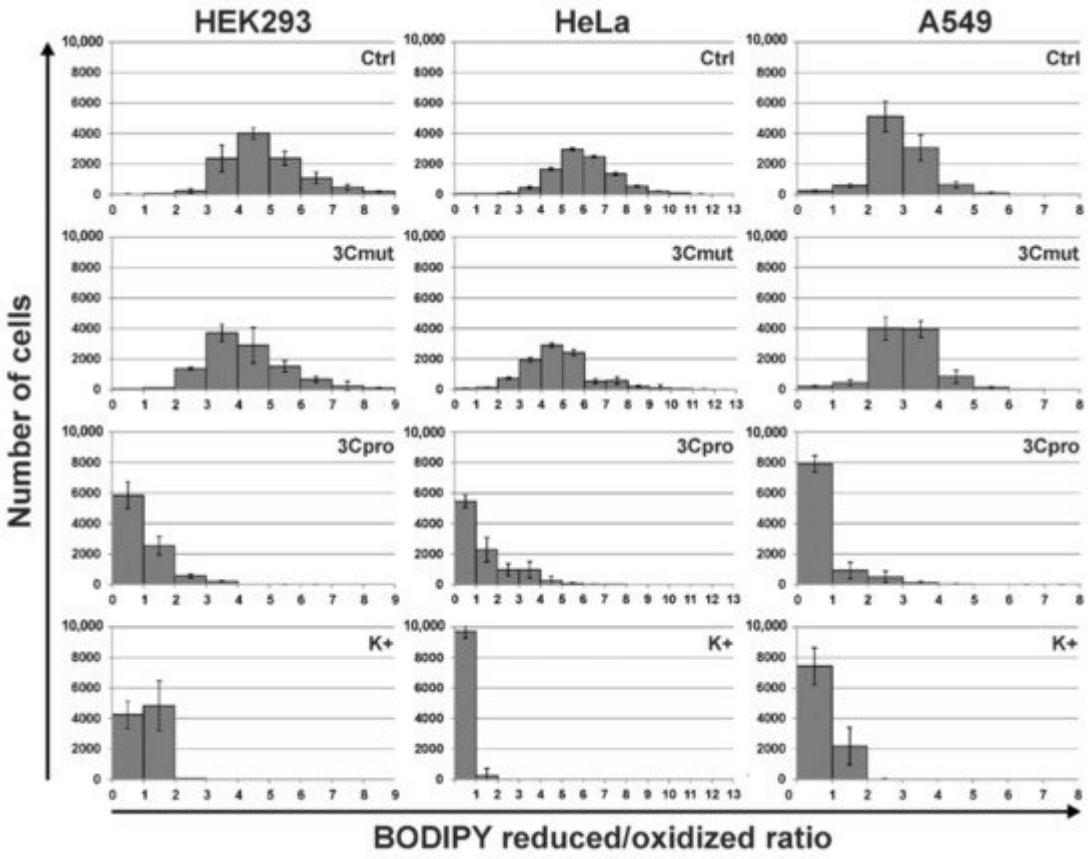

Figure 6. Lipid peroxidation upon 3Cpro/3Cmut expression. Non-transfected HEK293, HeLa, and A549 cells (Ctrl), transfected with pCI-3Cmut (3Cmut) or pCI-3C (3Cpro), and exposed to cumene hydroperoxide (K+) were incubated with BODIPY 581/591 C11 reagent, and analyzed using flow cytometry. For each cell in the population, the ratio of the fluorescence intensities of reduced (red) to oxidized (green) forms of BODIPY 581/591 C11 reagent were calculated. Values are represented as mean ± SD of two independent experiments with triplicates (*n* = 6).

Taken together, the results obtained indicate that 3Cpro-induced cell death is caused by active lipid peroxidation, and iron ions contribute to its progression. In turn, this allows us to conclude that the 3Cpro-induced cell death represents a form of ferroptosis. In general, the morphology of the cells died due to 3Cpro action is consistent with the ferroptotic one. Recent studies have shown that cells undergoing ferroptosis are usually characterized by necrosis-like morphological changes, including loss of plasma membrane integrity, cytoplasmic swelling (oncosis), swelling of cytoplasmic organelles and moderate chromatin condensation (reviewed in [25]). All these features have been found in cells expressing 3Cpro both in the current and in previous studies [11].

To date, numerous data indicate that different proteases can induce RCD; however, 3Cpro is the first reported proteolytic enzyme inducing ferroptosis. Moreover, all currently known specific ferroptosis inducers are synthetic low-molecular-weight compounds [26]. The found 3Cpro ability suggests this protease as a promising genetic ferroptosis-inducing agent, e.g., in cancer gene therapy. A wide range of cancer cells proved sensitive to ferroptosis; in particular, prostate, liver, lung, mammary

gland, pancreas cancer as well as glioblastoma, acute myeloid leukemia, and diffuse B-cell lymphoma (reviewed in detail in [27][28]).

However, the data obtained are not enough to establish the biological role of 3Cpro as a ferroptosis inducer. It is common knowledge that human hepatitis A virus has no direct cytopathic effect on hepatocytes, although the liver is the primary locus of virus replication. *In vivo* the main factor that damages the liver is the death of infected hepatocytes mainly due to the activity of cytotoxic T cells and natural killer cells [29][30]. Moreover, the intracellular level of 3Cpro is apparently much lower during the infection compared to that in our experimental system. In this context, it is likely that 3Cpro affects certain cell substrates to maintain viral replication *in vivo*, while ferroptosis induction is a side effect of 3Cpro action. Apparently, low cellular levels of 3Cpro have no such side effect, while higher protease levels in our experimental system can induce it. A detailed analysis of the molecular mechanism of 3Cpro-induced cell death is needed to reveal the relationship between the ability of 3Cpro to induce ferroptosis and the viral life cycle. In the first place, the cellular targets of 3Cpro should be identified. This information can also extend our knowledge about the mechanism and biological role of ferroptosis.

References

1. Allocati, N.; Masulli, M.; Di Ilio, C.; De Laurenzi, V. Die for the community: An overview of programmed cell death in bacteria. Cell Death Dis. 2015, 6, e1609.
2. Fuchs, Y.; Steller, H. Programmed Cell Death in Animal Development and Disease. Cell 2011, 147, 742–758.
3. Galluzzi, L.; Vitale, I.; Aaronson, S.A.; Abrams, J.M.; Adam, D.; Agostinis, P.; Alnemri, E.S.; Altucci, L.; Amelio, I.; Andrews, D.W.; et al. Molecular mechanisms of cell death: Recommendations of the Nomenclature Committee on Cell Death 2018. Cell Death Differ. 2018, 25, 486–541.
4. Laitinen, O.; Svedin, E.; Kapell, S.; Nurminen, A.; Hytönen, V.; Flodström-Tullberg, M. Enteroviral proteases: Structure, host interactions and pathogenicity. Rev. Med. Virol. 2016, 26, 251–267.
5. Sun, D.; Chen, S.; Cheng, A.; Wang, M. Roles of the Picornaviral 3C Proteinase in the Viral Life Cycle and Host Cells. Viruses 2016, 8, 82.
6. Calandria, C.; Irurzun, A.; Barco, A.; Carrasco, L. Individual expression of poliovirus 2Apro and 3Cpro induces activation of caspase-3 and PARP cleavage in HeLa cells. Virus Res. 2004, 104, 39–49.
7. Li, M.-L.; Hsu, T.-A.; Chen, T.-C.; Chang, S.-C.; Lee, J.-C.; Chen, C.-C.; Stollar, V.; Shih, S.-R. The 3C Protease Activity of Enterovirus 71 Induces Human Neural Cell Apoptosis. Virology 2002, 293, 386–395.

8. Chau, D.H.W.; Yuan, J.; Zhang, H.; Cheung, P.; Lim, T.; Liu, Z.; Sall, A.; Yang, D. Coxsackievirus B3 proteases 2A and 3C induce apoptotic cell death through mitochondrial injury and cleavage of eIF4GI but not DAP5/p97/NAT1. Apoptosis 2006, 12, 513–524.
9. Lötzerich, M.; Roulin, P.S.; Boucke, K.; Witte, R.; Georgiev, O.; Greber, U.F. Rhinovirus 3C protease suppresses apoptosis and triggers caspase-independent cell death. Cell Death Dis. 2018, 9, 1–18.
10. Shubin, A.V.; Lunina, N.A.; Shedova, E.N.; Roshina, M.P.; Demidyuk, I.V.; Vinogradova, T.V.; Kopantsev, E.P.; Chernov, I.P.; Kostrov, S.V. Evaluation of the toxic effects evoked by the transient expression of protease genes from human pathogens in HEK293 cells. Appl. Biochem. Microbiol. 2013, 49, 750–755.
11. Shubin, A.V.; Demidyuk, I.V.; Lunina, N.A.; Komissarov, A.A.; Roschina, M.P.; Leonova, O.G.; Kostrov, S.V. Protease 3C of hepatitis A virus induces vacuolization of lysosomal/endosomal organelles and caspase-independent cell death. BMC Cell Biol. 2015, 16, 4.
12. Shubin, A.V.; Komissarov, A.A.; Karaseva, M.A.; Padman, B.S.; Kostrov, S.V.; Demidyuk, I.V. Human hepatitis A virus 3C protease exerts a cytostatic effect on Saccharomyces cerevisiae and affects the vacuolar compartment. Biologia 2021, 76, 321–327.
13. Komissarov, A.; Karaseva, M.A.; Safina, D.R.; Roschina, M.P.; Bednova, O.P.; Kazakov, A.A.; Demkin, V.V.; Demidyuk, I.V. Comparative evaluation of the transgene expression efficiency provided by the model genetic constructs of different structure. Mol. Genet. Microbiol. Virol. 2016, 31, 156–162.
14. Komissarov, A.; Demidyuk, I.; Safina, D.; Roschina, M.; Shubin, A.; Lunina, N.; Karaseva, M.; Kostrov, S. Cytotoxic effect of co-expression of human hepatitis A virus 3C protease and bifunctional suicide protein FCU1 genes in a bicistronic vector. Mol. Biol. Rep. 2017, 44, 323–332.
15. Western Blot Normalization Using Image Lab Software, Quick Start Guide. Bio-Rad Bulletin 6434; Bio-Rad Laboratories: Hercules, CA, USA, 2015.
16. Bertrand, R.; Solary, E.; O'Connor, P.; Kohn, K.W.; Pommier, Y. Induction of a Common Pathway of Apoptosis by Staurosporine. Exp. Cell Res. 1994, 211, 314–321.
17. Degterev, A.; Huang, Z.; Boyce, M.; Li, Y.; Jagtap, P.; Mizushima, N.; Cuny, G.D.; Mitchison, T.J.; Moskowitz, M.A.; Yuan, J. Chemical inhibitor of nonapoptotic cell death with therapeutic potential for ischemic brain injury. Nat. Chem. Biol. 2005, 1, 112–119.
18. Jagtap, P.; Soriano, F.; Virág, L.; Liaudet, L.; Mabley, J.; Szabó, É.; Haskó, G.; Marton, A.; Lorigados, C.B.; Gallyas, F.; et al. Novel phenanthridinone inhibitors of poly(adenosine 5′-diphosphate-ribose) synthetase: Potent cytoprotective and antishock agents. Crit. Care Med. 2002, 30, 1071–1082.

19. Kajitani, K.; Fujihashi, M.; Kobayashi, Y.; Shimizu, S.; Tsujimoto, Y.; Miki, K. Crystal structure of human cyclophilin D in complex with its inhibitor, cyclosporin A at 0.96-Å resolution. Proteins Struct. Funct. Bioinform. 2007, 70, 1635–1639.
20. Zilka, O.; Shah, R.; Li, B.; Angeli, J.P.F.; Griesser, M.; Conrad, M.; Pratt, D.A. On the Mechanism of Cytoprotection by Ferrostatin-1 and Liproxstatin-1 and the Role of Lipid Peroxidation in Ferroptotic Cell Death. ACS Cent. Sci. 2017, 3, 232–243.
21. Angeli, J.P.F.; Shah, R.; Pratt, D.A.; Conrad, M. Ferroptosis Inhibition: Mechanisms and Opportunities. Trends Pharmacol. Sci. 2017, 38, 489–498.
22. Dixon, S.J.; Lemberg, K.M.; Lamprecht, M.R.; Skouta, R.; Zaitsev, E.M.; Gleason, C.E.; Patel, D.N.; Bauer, A.J.; Cantley, A.M.; Yang, W.S.; et al. Ferroptosis: An Iron-Dependent Form of Nonapoptotic Cell Death. Cell 2012, 149, 1060–1072.
23. Dolma, S.; Lessnick, S.L.; Hahn, W.C.; Stockwell, B.R. Identification of genotype-selective antitumor agents using synthetic lethal chemical screening in engineered human tumor cells. Cancer Cell 2003, 3, 285–296.
24. Yang, W.S.; Stockwell, B.R. Synthetic Lethal Screening Identifies Compounds Activating Iron-Dependent, Nonapoptotic Cell Death in Oncogenic-RAS-Harboring Cancer Cells. Chem. Biol. 2008, 15, 234–245.
25. Tang, D.; Chen, X.; Kang, R.; Kroemer, G. Ferroptosis: Molecular mechanisms and health implications. Cell Res. 2021, 31, 107–125.
26. Feng, H.; Stockwell, B.R. Unsolved mysteries: How does lipid peroxidation cause ferroptosis? PLoS Biol. 2018, 16, e2006203.
27. Lu, B.; Chen, X.B.; Ying, M.D.; He, Q.J.; Cao, J.; Yang, B. The Role of Ferroptosis in Cancer Development and Treatment Response. Front. Pharmacol. 2018, 8, 992.
28. Shen, Z.; Song, J.; Yung, B.C.; Zhou, Z.; Wu, A.; Chen, X. Emerging Strategies of Cancer Therapy Based on Ferroptosis. Adv. Mater. 2018, 30, e1704007.
29. Fleischer, B.; Fleischer, S.; Maier, K.; Wiedmann, K.H.; Sacher, M.; Thaler, H.; Vallbracht, A. Clonal analysis of infiltrating T lymphocytes in liver tissue in viral hepatitis A. Immunology 1990, 69, 14–19.
30. Baba, M.; Hasegawa, H.; Nakayabu, M.; Fukai, K.; Suzuki, S. Cytolytic activity of natural killer cells and lymphokine activated killer cells against hepatitis A virus infected fibroblasts. J. Clin. Lab. Immunol. 1993, 40, 47–60.